REVISION
22nd April 2014

One-Step Preparation of the $BiVO_4$ Film Photoelectrode

Lucia H. Mascaro [a,b*], Adam Pockett [a], John M. Mitchels [a], Laurence M. Peter [a], Petra J. Cameron [a], Veronica Celorrio [c], David J. Fermin [c], Jagdeep S. Sagu [d], K.G. Upul Wijayantha [d], Gabriele Kociok-Köhn [a], and Frank Marken [a*]

[a] *Department of Chemistry, University of Bath, Bath BA2 7AY, UK.*
[b] *Department of Chemistry, San Carlos Federal University, Rod. Washigton Luiz, km235, CEP 13565-905, São Carlos, SP - Brazil.*
[c] *School of Chemistry, University of Bristol, Bristol BS8 1TS, Avon, England.*
[d] *Department of Chemistry, University of Loughborough, Loughborough LE11 3TU, Leicestershire, England.*

to be submitted to
Journal of Solid State Electrochemistry
Special Issue in memorial of Professor Lothar Dunsch

Proofs to F. Marken
(F.Marken@bath.ac.uk)

Abstract

A one-step method of preparing photo-electrochemically active nano-structured $BiVO_4$ films is reported based on thermolysis (500 ºC in air) of a poly-ethyleneglycol (PEG300) "paint-on" precursor solution containing Bi^{3+} (as nitrate) and VO_4^{3-} (as the metavanadate ammonium salt). Films are formed directly on tin-doped indium oxide (ITO) substrates and characterised by electron microscopy (SEM, EDS), X-ray diffraction, Raman spectroscopy, and photo-electrochemistry. The nanocrystalline film exhibited typically up to 52% incident photon to current efficiency (IPCE) at 1.0 V vs. SCE in aqueous 0.5 M Na_2SO_4 with oxalate, strongly enhancing photocurrents.

Keywords: water splitting, photoanode, oxygen evolution, solar energy, vanadium oxide, nanostructure.

1. Introduction

Bismuth vanadate ($BiVO_4$) is an n-type semiconductor, which is usually used as a yellow pigment, but which has recently also attracted attention for use in photoelectrochemical water splitting [1-4] and in the photolytic destruction of organic pollutants [5, 6]. The advantages offered by $BiVO_4$ are (i) a suitable band gap (usually 2.4 to 2.5 eV for monoclinic $BiVO_4$, however, a wider range of values has been reported), (ii) inexpensive components, and (iii) excellent stability in aqueous media, making this material a promising photoanode for visible light harvesting. More recent studies have focused on the preparation of $BiVO_4$, seeking to improve photocatalytic activity by using various strategies such as morphology control, construction of nano-composite structures, and doping. $BiVO_4$ can be fabricated by solution-based methods including aqueous, hydrothermal, and solvothermal processes [7-9] or by spray pyrolysis [10]. In most of the synthesis methods proposed in the literature, several hours of reflux and use of aggressive chemicals such as concentrated nitric acid are required. In addition, often $BiVO_4$ is obtained as powder material, and when it is employed in photo-electrodes an extra preparation step (conversion of powder to thin film) is necessary. For example, an elegant solvothermal method using an ethylene glycol–water–sodium oleate system was proposed by Wang et al. where the precursor solution was treated in a Teflon-lined autoclave at 180^o C for 24 h and $BiVO_4$ powder was produced [11]. Sayama et al. used a modified method of metal-organic decomposition and a poly-ethyleneglycol solvent followed by evaporation under vacuum to obtain $BiVO_4$ films on ITO [12]. In this paper we propose a

relatively simple and direct one-step route to photo-active $BiVO_4$ nanostructured films based on combining $Bi(NO_3)_3$ and NH_4VO_3 directly in poly-ethyleneglycol (PEG300) as solvent, and applying this precursor solution to ITO coated glass, followed by thermal treatment at 500 ^oC in air.

2. Experimental

Reagents used were $Bi(NO_3)_3{\cdot}5H_2O$, NH_4VO_3, poly-ethylene glycol (PEG300) and Na_2SO_4 from Sigma-Aldrich (UK). Aqueous solutions were prepared with deionized and filtered water taken from a Thermo Scientific water purification system (Barnstead Nanopure, UK). Electrochemical measurements were performed with a μAutolab Type II potentiostat system (Ecochemie, Utrecht, NL) with Autolab GPES software.

A solar simulator Xe lamp with 100 mW cm^{-2} (AM1.5) output was employed in cyclic voltammetry photo-electrochemical experiments. In some experiments a high power blue LED (λ = 405 nm, M405L2 UV LED, Thorlabs, Ely, UK) together with LED driver (T-Cube LED driver, Thorlabs, Ely, UK) and a DDS Function/Arbitrary TG4001 Generator (TTi, Huntingdon, UK) were employed. The electrode/electrolyte contact area was 1 cm^2, front-lit, and the electrolyte was 0.5 M Na_2SO_4. Field emission scanning electron microscopy (FE-SEM) images were obtained using a JEOL JSM6301F microscope. Photocurrent spectra (incident photon-to-current efficiency, IPCE data) were plotted as a function of incident light with λ ranging from 350 to 550 nm in steps of 10 nm. Light intensity of this optical window was calibrated using a standard silicon photodiode. The

light chopping frequency was set at 0.5 Hz to minimise the attenuation affects. The apparatus was based on a Stanford Research Systems SR830 (Stanford, US) lock in amplifier, SR540 chopper controller, a homemade potentiostat, a 75 W xenon lamp powered by a Bentham 650 (Reading, UK) power supply, and a mono-chromator controller PMC3B of Bentham Instruments Ltd. (Reading, UK). Raman spectroscopy studies were carried out with an inVia Renishaw Raman microscope system (Gloucestershire, UK). The crystal phase of $BiVO_4$ thin film was confirmed by X-ray diffraction (XRD, Bruker AXS D8 Advance diffractometer with a θ-2 θ configuration and using CuKα radiation λ = 1.5418 Å). Diffuse reflectance spectra were obtained using a UV-Vis-NIR spectrometer (Perkin Elmer Lambda 35).

The electrodes used were a platinum wire counter electrode and a potassium chloride saturated calomel (SCE) reference electrode. The working electrodes were made from tin-doped indium oxide (ITO, Image Optics Components, Basildon, Essex, UK) coated glass, cut to give 1 cm × 3 cm electrodes (sonicated at 30 min in acetone and washed distilled water and heated 1 h at 500^o C before use).

For $BiVO_4$ film production, initially two solutions were prepared. The first solution was prepared by dissolving 1.036 g of $Bi(NO_3)_3{\cdot}5H_2O$ in 5 mL of PEG300 and the second by dissolving 0.25 g of NH_4VO_3 in 5 mL of PEG300. The solutions were then mixed to form a dark orange solution, which was agitated in an ultrasonic bath for 30 minutes. This mixture was then used as the precursor for deposition of $BiVO_4$ films. The deposition was carried out by employing a drawing roller (hard rubber lino printing roller) [13]. The

precursor solution was distributed evenly onto the ITO substrate (ca. 20 μL cm^{-2} to give an average thickness of 0.2 to 0.5 μm) and it was then pre-dried with warm air for 15 minutes. The process was repeated to increase the thickness of the film. After this deposition, the coated ITO was heated at 500° C (this temperature was chosen to give high quality $BiVO_4$ films without deformation of the underlying glass slide) for 1 hour in a tube furnace in presence of air. The ITO glass film substrate was fully covered with a yellow and adherent film after the preparation process.

3. Results and Discussion

The Raman spectrum and XRD data for $BiVO_4$ thin films are shown in Figure 1A and 1B, respectively. From the Raman data it is possible to observe characteristic peaks at around 210, 324, 368, 720 and 828 cm^{-1}, corresponding to the Raman active vibrational modes consistent with a pure monoclinic phase film of $BiVO_4$ [14]. The appearance of V-O band at 828 cm^{-1} indicates good crystallinity [15,16]. The broad peak at 1100 cm^{-1} corresponds to the ITO substrate. Figure 1B shows the XRD pattern for the $BiVO_4$ film sample. The indexed peaks are associated mainly with the planes of the monoclinic $BiVO_4$ structure (PDF No 01-083-1699). The characteristic strong peak of tetragonal zircon phase at 24° was not observed, and therefore, there is no tetragonal zircon-type $BiVO_4$ phase present in the samples [17]. It is also possible to observe further diffraction peaks from the underlying ITO substrate, identified with an asterisk symbol in Figure 1B. A scanning electron micrograph (SEM) of a $BiVO_4$ film is shown in Figure 1C, where agglomeration of individual crystallites is observed. The SEM image shows that the film is dense,

crystalline, and with particles typically around 1 to 2 μm in diameter. The energy-dispersive X-ray spectroscopy (EDS) data analysis (Figure 1 D) revealed the presence of the elements Bi, V, and O in the film with approximately 1:1 atomic ratio for Bi:V.

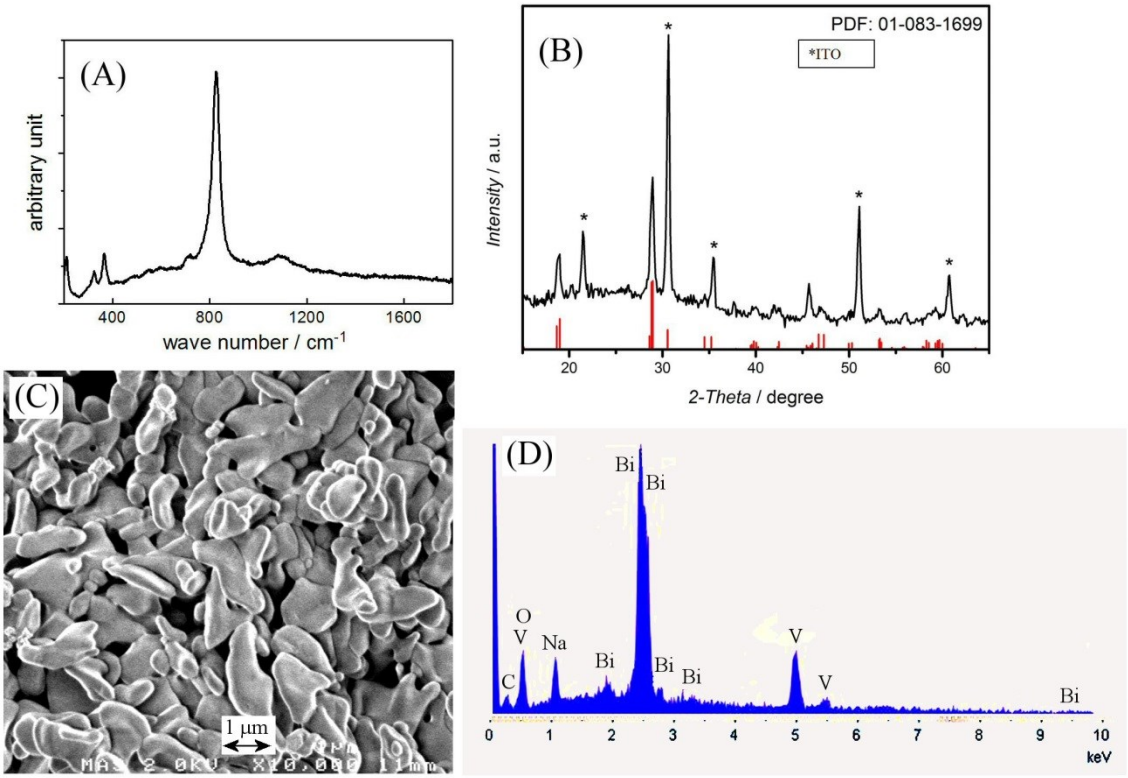

Figure 1. (A) Raman spectrum, (B) X-ray diffraction pattern, and (C) FE-SEM image with (D) EDS analysis for the $BiVO_4$ thin film electrode formed on ITO.

Typical cyclic voltammograms for the $BiVO_4$ film on ITO in aqueous 0.5 M Na_2SO_4 solution in light and in the dark are shown in Figure 2A. Two characteristic redox systems centred at approximately -0.1 V (weak) and at -0.4 V vs. SCE (strong) are indicative of reduction and re-oxidation of two different types of V^{5+} to V^{4+} surface states

(tentatively assigned; or possibly also accumulation of charges in the conduction band, which has been reported to have mixed V, Bi, and O character [18,7]). An anodic photo-current is observed commencing from ca. 0.0 V vs. SCE, which increases with increased bias potential when under illumination. The anodic photocurrent is associated with photo-oxidation of water. Hysteresis in the photo-current profile is likely to be linked to local pH changes within the porous film structure. At 1.0 V vs. SCE a typical value for the photocurrent is 300 $\mu A\ cm^{-2}$ under solar simulator conditions (AM1.5). Substantially lower photocurrents were reported for example by Chatchai et al. using FTO/SnO_2/$BiVO_4$ and FTO/$BiVO_4$ film photoanodes [19]. The photocurrent observed in this work is larger than most results reported in the literature for pure $BiVO_4$ films [19-21] and consistent with high-quality films with good electrical contact to the underlying substrate.

The diffuse reflectance spectra of the samples were measured (see Figure 2B). The band gap can be estimated as 2.52 eV (see red line), which is close to the values reported previously [10, 11, 13, 17]. In contrast, tetragonal zircon type $BiVO_4$ has been reported to exhibit a wider less beneficial band gap (2.9 eV) [18]. Therefore the results are consistent with Raman and XRD data, which indicate the presence of only the monoclinic $BiVO_4$ phase. In Figure 2C, the IPCE values for $BiVO_4$/ITO electrodes are presented as a function of the irradiation wavelength measured at +1.0 V vs. SCE anodic bias in 0.5 M Na_2SO_4 solution. The electrodes show photocurrent responses in the visible-light region up to about 490 nm (see inset) in accordance the literature. Again a band gap of approximately 2.52 eV (see red line) characteristic of $BiVO_4$ is observed. The ITO/$BiVO_4$ electrode shows a high efficiency for solar light conversion in both regions of UV and visible light. The

maximum value of IPCE was 52%, which is considerable when compared to typical results reported in the literature [19-23], but lower than the 73% IPCE data (at 420 nm) reported by Jie et al. [24].

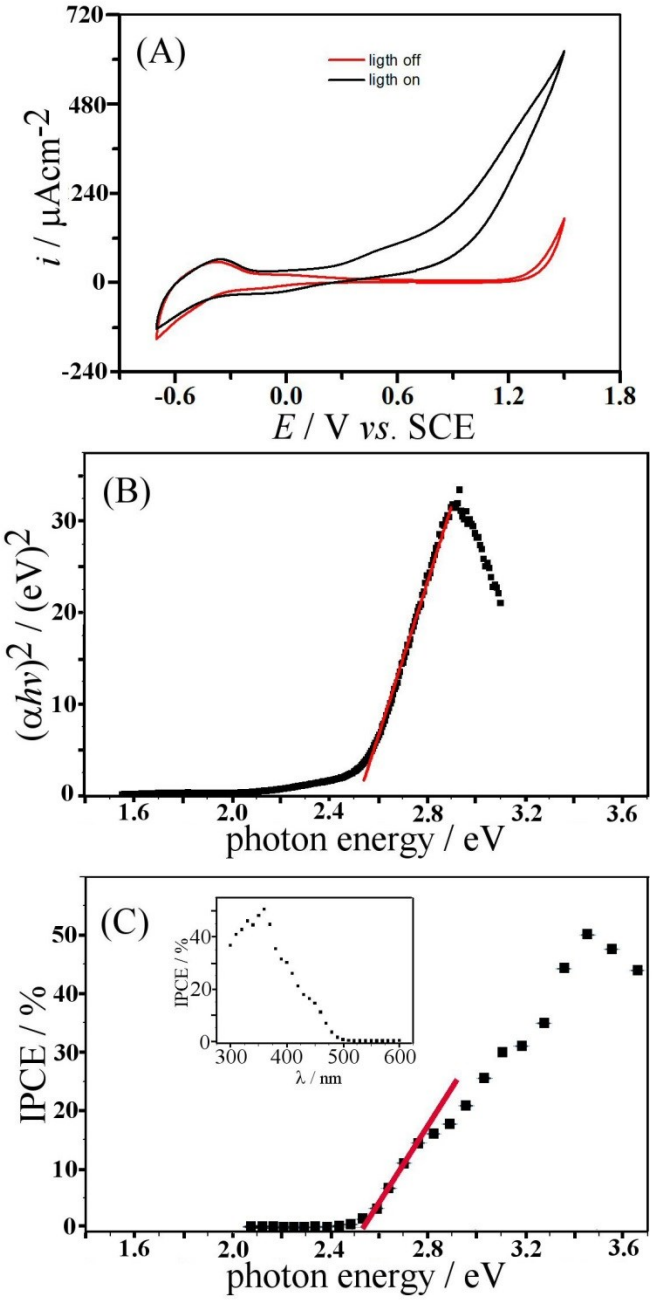

Figure 2. (A) Cyclic voltammetry (scan rate 20 mVs^{-1}) for a $BiVO_4$ film electrode in 0.5 M Na_2SO_4 in the dark and light (AM1.5 solar simulator, 100 $mWcm^{-2}$ Xe lamp). (B) Diffuse reflectance data plot $(\alpha h\nu)^2$ versus photon energy for a $BiVO_4$ thin film on ITO. (C) IPCE plot for a $BiVO_4$ thin film at 1.0 V vs. SCE in 0.5 M Na_2SO_4. Inset: IPCE plot versus wavelength.

Both, this study and that by Jie et al. [24] are based on a thermolysis processes involving a precursor solution, which may have beneficial effects on the resulting substrate to $BiVO_4$ film interface. This interface is crucial in allowing effective flow of electrons into the underlying ITO substrate as well as in minimising recombination by oxygen reacting with V(IV) or directly at the ITO surface. The nature of this interface is likely to be affected by the gradual evaporation of PEG and residual components forming during thermolysis.

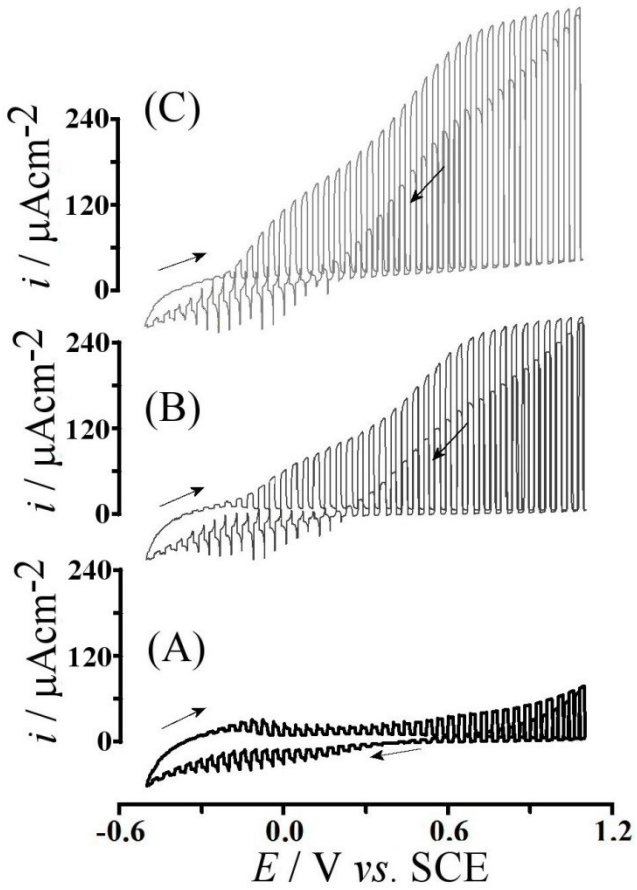

Figure 3. (A-C) Cyclic voltammetry (scan rate 20 mVs^{-1}) for a $BiVO_4$ film electrode in 0.5 M Na_2SO_4 (A) with 8 mM oxalate (B) and with 50 mM oxalate (C) in the presence of pulsed light (blue LED, 0.5 Hz).

The presence of recombination processes can be demonstrated by addition of oxalate hole quencher into the aqueous phase and study of photocurrents under pulsed blue light conditions. Figure 3 shows data for (A) a $BiVO_4$ electrode immersed in 0.5 M Na_2SO_4, (B) the same experiment in the presence of 8 mM oxalate, and (C) in the presence of 50 mM oxalate (all at pH 5). In the absence of oxalate a typical light pulse transient response is observed with cross-over from anodic to cathodic photo-current pulse depending on the scan direction. This behaviour suggests non-steady state behaviour possibly due to pH gradients developing in the solution close to the electrode surface. With 8 mM oxalate present (Figure 3B), features are similar, but now significantly higher photocurrents are detected. Oxalate is able to react with two holes from the photo-excited $BiVO_4$ to give CO_2 [25] (this is possible even on the ITO substrate [26] but the process is believed to be dominated here by $BiVO_4$). Therefore recombination via solution processes can be suppressed. Further increase in oxalate concentration to 50 mM (see Figure 3C) causes only minor further enhancement. There are two distinct steps in the photocurrent possibly due to the increase in applied bias potential causing a change in reaction pathway. Even higher concentrations of oxalate were observed to gradually corrode $BiVO_4$ (presumably by extraction of Bi^{3+} cations) associated with an increase in the dark current.

4. Conclusions

A crystalline, homogeneous, and adherent $BiVO_4$ thin film with monoclinic structure was produced on ITO substrate electrodes using a one-step method based on a PEG300 precursor solution. The method is experimentally simple, fast, and inexpensive,

and leads to an effective ITO-$BiVO_4$ interface. The photo-anode material obtained exhibits photocurrents over a large potential range and with good IPCE values. It can be concluded that the "paint-on" synthesis of $BiVO_4$ films presented in this work is promising for use as photoelectrodes in water splitting, in photocatalytic degradation of organics, or in dye-sensitised solar cells [27]. Work on a wider range of substrates and applications is in progress.

Acknowledgements

LHM thanks FAPESP (proc. 2012/23422-5). VC gratefully acknowledges the UK National Academy for support through the Newton International Fellows program. We thank the EPSRC for funding (DTC studentship for Adam Pockett, Grant EP/G03768X/1).

References

[1] Ding C, Shi J, Wang D, Wang Z, Wang N, Liu G, Xiong F, Li C (2013) Phys Chem Chem Phys 15: 4589-4595.
[2] Saito R, Miseki Y, Sayama K (2013) J Photochem Photobio A: Chem 258: 51– 60.
[3] Pilli SK, Deutsch TG, Furtak TE, Brown LD, Turner JA, Herring AM (2013) Phys Chem Chem Phys 15: 3273-3278.
[4] Jeong HW, Jeon TH, Jang JS, Choi W, Park H (2013) J Phys Chem C 117: 9104-9112.
[5] Shi W, Yan Y, Yan X (2013) Chem Engineer J 215: 740-746.
[6] da Silva MR, Dall'Antonia LH, Scalvi LVA, dos Santos DI, Ruggiero LO, Urbano A (2012) J Solid State Electrochem 16: 3267-3274.
[7] Park Y, McDonald KJ, Choi KS (2013) Chem Soc Rev 42: 2321-2337.
[8] Zhang J, Luo W, Li W, Zhao X, Xue G, Yu T, Zhang C, Xiao M, Li Z, Zou Z (2012) Electrochem Commun 22: 49-52.
[9] Myung N, Ham S, Choi S, Chae Y, Kim WG, Jeon YJ, Paeng KJ, Chanmanee W, de Tacconi NR, Rajeshwar K (2011) J Phys Chem C 115: 7793-7800.
[10] Li MT, Zhao L, Guo L (2010) Int J Hydrogen Energy 35: 7127-7133.

[11] Wang X, Li G, Ding J, Peng H, Chen K (2012) Mater Res Bull 47: 3814-3818.
[12] Sayama K, Nomura A, Zou Z, Abe R, Abe Y, Arakawa H (2003) Chem Commun 2908-2909.
[13] Ahmed S, Hassan IAI, Roy H, Marken F (2013) J Phys Chem C 117: 7005-7012.
[14] Frost RL, Henry DA, Weier ML, Martens W (2006) J Raman Spectroscopy 37: 722-732.
[15] Yao MM, Liu MX, Gan LH, Zhao FQ, Fan XZ, Zhu DZ, Xu ZJ, Hao ZX, Chen LW (2013) Coll Surf A-Physicochem Engineer Aspects 433: 132-138.
[16] Kho YK, Teoh WY, Iwase A, Mädler L, Kudo A, Amal R (2011) Appl Mater Interfaces 3: 1997-2004.
[17] Luo W, Wang Z, Wan L, Li Z, Yu T, Zou Z (2010) J Phys D: Appl Phys 43: 405402.
[18] Walsh A, Yan Y, Huda MN, Al-Jassim MM, Wei SH (2009) Chem Mater 21: 547-551.
[19] Chatchai P, Murakami Y, Kishioka SY, Nosaka AY, Nosaka Y (2008) Electrochem Solid State Lett 11: H160-H163.
[20] Abdi FF, Firet N, van de Krol R (2013) ChemCatChem 5: 490-496.
[21] Nagabhushana GP, Nagaraju G, Chandrappa GT (2013) J Mater Chem A 1: 388-394.
[22] Liu H, Nakamura R, Nakato Y (2005) J Electrochem Soc 152: G856-G861.
[23] Zhou M, Bao J, Bi W, Zeng Y, Zhu R, Tao M, Xie Y (2012) ChemSusChem 5: 1420-1425.
[24] Jia QX, Iwashina K, Kudo A (2012) PNAS 109: 11564-11569.
[25] Byrne JA, Eggins BR (1998) J Electroanal Chem 457: 61-72.
[26] Tansil NC, Xie H, Gao, ZQ (2004) J Phys Chem B 108: 16850-16854.
[27] Dong W, Guo YP, Guo B, Li H, Liu HZ, Joel TW (2013) ACS Appl Mater Interfaces 5: 6925-6929.